

# Role of Heat Treatments on Phase Decomposition and Microstructure Morphology Impact on Mechanical Properties of High Strength Steel

<sup>1</sup>Enefola S. Ameh, <sup>2</sup>Basil O. Onyekpe

<sup>1</sup>Mechanical Department, University of Benin, Nigeria

<sup>2</sup>Mechanical Department, University of Benin, Nigeria

**Abstract**—The research work studied the role of heat treatments on phase decomposition and microstructure morphology impact on fracture toughness, yield strength and hardness of high strength steel. Normalizing, austempering and quenching and tempering were performed after initial austenization of the as-received steel to 950°C at 90mins isothermal holding period and the respective microstructure characterized with light optical and scanning electron microscopes. J-integral, tensile and hardness tests were conducted in accordance with American standard test method E1820, E8 and E92 respectively. The results showed remarkable high fracture toughness, yield strength and hardness parameters sensitivity to microstructure morphology and quenched and tempered microstructure indicated the best mechanical properties combination trade off, followed by austempered, as-received and normalized microstructure.

**Keywords**— Fracture toughness, hardness, heat treatment, microstructure, yield strength.

## 1.0 INTRODUCTION

High strength steels are widely used in offshore environment such as platform leg tension, pressure vessel, pipelines and jacket structures owing to lower weight and lower manufacturing cost [1]. Fracture toughness, yield strength and hardness are fundamental mechanical properties considered in high strength steel design to overcome harsh offshore environment [2]. But the combination of these mechanical properties is usually difficult to attain because an increase in one of these properties leads to a decrease in the others [3]. High strength steel microstructures and its correlation to major mechanical properties remains complex and are being influenced by heat treatment process, homogeneousness and composition [4]. The impact of microstructure morphology on mechanical properties of high strength steel still have contradictory literatures because of complexity with microstructural phases, constituent formation mechanism including the fact that different microstructures offer different combination of toughness, strength and hardness for the same chemical composition [5].

## 2.0 LITERATURE SURVEY

Microstructural makeup and resultant mechanical properties depend on the heat treatment methods or cooling rates. Heat treatment has become an industrial process used to soften steel to change grain size, modify material structure and free induced-stress in a material [6]. It is a combination of heating usually to austenization temperature and then cooling in water, oil or air with a view to hardening or softening it [7]. The high temperature austenization phase in steel has the property to transform into mixture of two or more constituents like ferrite, pearlite, bainite, martensite and retained austenite depending on the cooling cycle [8]. The most widely used heat treatment processes include hardening, normalizing, annealing, quenching and tempering [9].

Microstructural constituents such as pro-eutectoid ferrite appearance at the grain boundaries which is usually formed at 520 – 720°C improves toughness properties of steel independent of heat treatment process [10]. Study has shown that impact fracture toughness of steel which had undergone normalization will probably yield tougher value than hardened and tempered steel [11]. While bainite microstructural constituent is believed to be formed during austempering heat treatment in the presence of Mo and Ni alloy elements which help to suppress pearlite reaction to allow austenite transformation to bainite. Lower bainite shape appeared more needle-like and formed within temperature range of 400 – 250°C while the upper bainite with feathery and broader plate appearance is usually formed with 500 – 400°C [12].

Mechanical properties and microstructures of mild steel subjected to annealed, normalized and hardened heat treatments at 850°C austenization temperature had been investigated and concluded that the hardness values of heat treated samples were all lower than the as-received which has ferrite-austenite duplex phase composition [13]. Similarly, examination of mechanical properties of medium carbon steel at the same initial austenization temperature for different heat treatment methods (normalizing, annealing, hardening and tempering) indicated annealed sample showed the lowest strength and hardness and highest ductility and toughness values but hardened samples indicated highest strength and hardness with lowest ductility and toughness values [14] and effect of heat treatment and mechanical properties of spring steel studied revealed decrease in hardness and strength but increased in ductility with increasing tempering temperature and time [15].

Several researches on heat treatments effect on microstructure and mechanical properties of carbon or spring steel have been carried out but rarely had work been done on high strength steel which has very complex microstructure owing to micro alloying elements. The present research work is aimed at examining the role of heat treatment on phase decomposition and impact of microstructure morphology on mechanical properties such as fracture toughness, strengths and hardness of high strength steel. The practical relevance of the work include further development of fundamental understanding of the complex high strength steel microstructure, improve mechanical properties trade off, material qualification and selection.

### 3.0 RESEARCH METHODOLOGY

#### 3.1 Material Heat Treatment and Characterization

25mm thick plate of high strength steel was procured from Masteel Company in UK. The chemical composition of the steel are - 0.0017% boron, 0.076% aluminum, 0.026% niobium, 0.004% titanium, 0.062% chromium, 0.002% vanadium, 0.11% molybdenum, 0.051% nickel, 0.0006% sulphur, 0.0042% nitrogen, 0.011% phosphorus, 0.03% copper, 0.296% silicon, 1.3% manganese, 0.161% carbon and the remainder percentage for iron. Samples were cut from bulk material and heated initially to 950°C austenization temperature and 90minute isothermal holding time and processed through normalization, austempering and quenching and tempering heat treatments as prescribed by ASM [16]. The samples for austempering were quenched from 950°C to 350°C salt bath in electric resistance furnace with 2mole potassium chloride and 1mole barium chloride and held for 90minutes before cooling in air. But the samples for quenching and tempering were tempered at 550°C after initially being quenched in water and normalized samples cooled in air to ambient temperature. Samples extracted were sectioned and encapsulated prior to progressive grinding with 120, 220, 600 and 1200 emery paper. The samples were further polished with 6micron and 1micron. The shining mirror-like specimen surfaces etched in 2% nital and then viewed under both light optical and scanning electron microscopes fitted with digital camera and computer system at an accelerated 15KV.

#### 3.2 J-integral Testing

Testing was carried out according to ASTM E1820. Specimens were machined to compact tension geometry (Fig 1) and dimensions as indicated Table 1. Each specimen was fatigue precracked to  $a/w$  of 0.5 and tested at room temperature using an Instron servo-hydraulic machine and automated computer controlled testing procedures. Load versus crack mouth opening displacement ( $v$ ) was plotted online and a compliance technique was employed in crack increment measurement using the following mathematical expressions [17]:

$$a_i/w = 1.00196 - 4.06319U + 11.242U^2 - 106.043U^3 + 464.335U^4 - 650.677 \quad (1)$$

Where,  $U = 1/\sqrt{BEC_i} + 1$ ,  $B$  = specimen thickness,  $C_i$  = compliance,  $E$  = Modulus of elasticity. But the crack mouth opening displacement ( $V$ ) which is a function of crack length increment was computed with mathematical relationship:

$$V = P [65.351 - 298.06 a/W + 630.11(a/W)^2]/EB \quad (2)$$

Where,  $P$  = applied load and  $W$  = specimen width

J-integral versus crack extension curves was plotted online to for each crack length increment in order to determine critical fracture toughness using the following equation:

$$J = k^2(1 - \nu^2)/E \left[ J_{pl(i-1)} + \left( \frac{\eta_{pl}}{B(i-1)} \right) (A_{pl(i)} - A_{pl(i-1)}) (1 - \gamma_{pl}) \left( \frac{a_i - a_{(i-1)}}{B(i-1)} \right) \right] \quad (3)$$

Where,  $k$  = stress intensity factor,  $A_{pl(i)} - A_{pl(i-1)}$  = increment of plastic area under load versus CMOD,  $J_{pl(i-1)}$  = initial plastic area under load versus CMOD and  $a_i - a_{(i-1)}$  = incremental crack length.

**Table 1: CT Specimen dimensions**

Quantity	Measured value (mm)
Specimen height (H)	1.2*W = 30.50
Specimen width (W)	25.40
Specimen thickness (B)	0.5*W = 12.70
Crack length (notch + pre-cracked)	$0.45 \leq a_o/W \leq 0.55$ .
Notch Length (n)	0.25*W = 6.35
Pre-cracking length (L)	0.05B = 0.64
Notch height (N)	0.1*W = 2.54
Span length (S)	0.55*W = 13.97
Pin hole diameter (d)	0.25*W = 6.35
Total specimen length (T)	1.25*W = 31.75

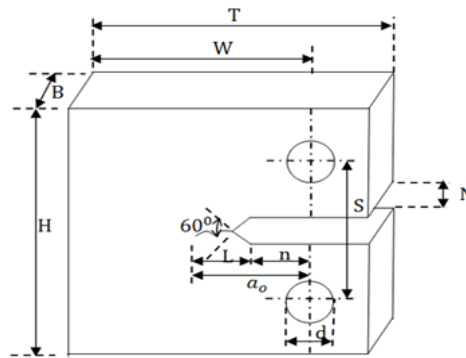


**Figure 1: CT specimen geometry**

### 3.3 Tensile Testing

Four specimens were extracted from bulk steel plate and machined to flat tensile specimen (Fig 2) and test conducted at ambient temperature according to ASTM E8 [18] at 1mm/s loading rate using automated controlled hydraulic testing machine and the elongation with corresponding loads recorded and stress – strain curves were automatically plotted on a computer controlled system.

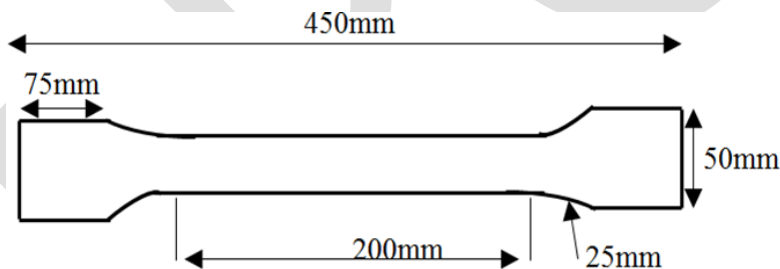


**Figure 2: Flat tensile specimen geometry**

### 3.4 Hardness Testing

Hardness test specimens were firstly cut from steel plate. Each specimen was encapsulated in a plastic for ease of handling and then polished on 1micron after grinding with several emery paper grades. The hardness test was performed using Vicker measuring technique with pyramidal diamond shaped tip indenter (Fig 3) which delivered load into the prepared surface of samples for a period of 14 seconds as prescribed by ASTM E92 [19]. 15kg load from the machine was applied to six different points on the test surface with indenter via weight lever and the vicker hardness value (Hv) calculated from the following mathematical expression:

$$HV = \frac{1.8544F}{d^2} \quad (4)$$

Where,  $F$  = applied load and  $d$  = diameter of indentation

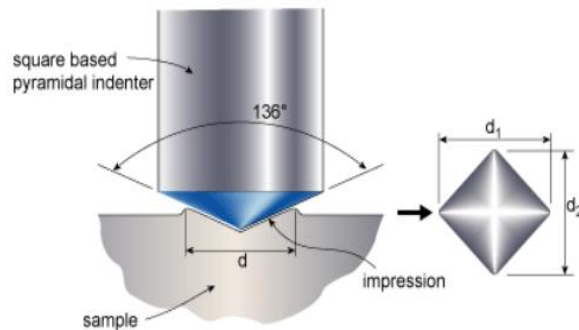


Figure 3: Vicker hardness test schematic [20]

## 4.0 RESULTS AND DISCUSSION

### 4.1 Role of Heat Treatments on Phase Decomposition

Microstructure (Fig 4) of the as-received exhibited complex arrangement of martensite with carbide precipitate distributed through the morphological structure and resemblance of the quenched and tempered microstructure indicating the as-received steel was probable produced through quenched and tempered heat treatment process. Normalization microstructure (Fig 5) had undergone complete recrystallization resulting in coarse ferrite/pearlite. The austenite partially transformed to pro-eutectoid ferrite, leaving the remaining carbon – enriched austenite transformed to pearlite during cooling. The microstructure micrograph revealed predominately pro-eutectoid ferrite matrix with interconnected and degenerated pearlite colonies at the grain boundaries. There was obvious coalescence and large interfacial between ferrite-pearlite structures but no evidence of ferrite/pearlite banding formation.

Resultant austempered microstructure (Fig 6) after austenizing the as-received steel to 950°C and austempering to 350°C for 90minutes time consisted basically short bainite sheaves and traces of coarse ferrite/pearlite grains presence. The micrograph showed bainite sheaves started deforming but the sheaves shapes were still much visible. The amount of bainite formed was believed to be largely depended on austenization temperature and time which determine austenite quantity available to transform to bainite and it is formed during austempering heat treatment in the presence of Mo and Ni alloy elements which help to suppress pearlite reaction to allow austenite transform into bainite. The bainite structure revealed traces of upper bainite with feathery and broad plate appearance at 350°C austempering temperature in the lower bainite structure and was not in agreement with [12] the finding that upper bainite which is associated with feathering and broad appearance plate is usually formed within the temperature range of 500°C to 400°C. The lower bainite structure probably contained traces of upper bainite owing to the long austempering duration of 90minutes agreed with the [21] study that austempering duration extending beyond 15 to 25minutes lead to bainite structure coarsening phenomenon because of the austenite grain growth which consequently yielded thick and feathering bainite structure. The traces of ferrite/pearlite in the austempered microstructure may have resulted from incomplete transformation of austenite to bainite due to quenching and consequently resulted in some austenite transformation to ferrite/pearlite and the remaining untransformed austenite was trapped in the bainite matrix as retained austenite at room temperature. The volume fraction of ferrite depend largely on these transformation kinetics and it is known to increase and coarser with increasing austempering temperature.

The quenched and tempered microstructure (Fig 7) at 550°C for 90minutes austenization time clearly showed large packets and blocks of martensite structure with recrystallized ferrite grains as the white region. Microstructure of high strength steel consisted martensite/bainite matrix after austenization to 950°C and quenched. The matrix exhibited tempered martensite/bainite microstructure after tempering [22]. The tempered martensites contain ferrite with carbide precipitates within and at the boundaries of the laths. The tempered martensite structure produced coarse grain and well dispersed carbide precipitates in white ferrite region matrix [23] depending on the soaking time. Particle sizes increased due to long tempering time that permitted more precipitates, carbon diffused far and spacing of the of the carbon rich phase  $Fe_3C$  become larger.

But the as-received, austempered, quenched and tempered microstructures showed some light coloured regions probably representing retained austenite. Austenite is known to exist in normal phase at high temperature but retained austenite becomes unstable below the range of normal temperature and could be harmful to mechanical properties when the content is greater than 15%. Therefore the retained austenite will change to martensite if significant drop in temperature lower than the temperature to which it was quenched is allowed or if the room temperature austenite is allowed to undergo high level mechanical stress. This transformation is



usually accompanied with volume change or geometry within the internal structure that may induce internal stress and manifest itself as crack [24].

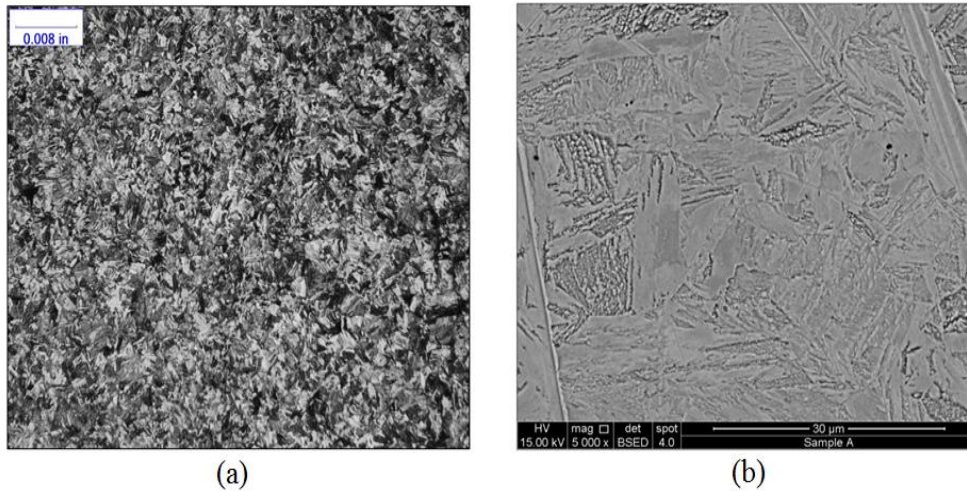


**Figure 4:** Microstructure of the as-received sample –a) LOM X200, b) SEM X5000

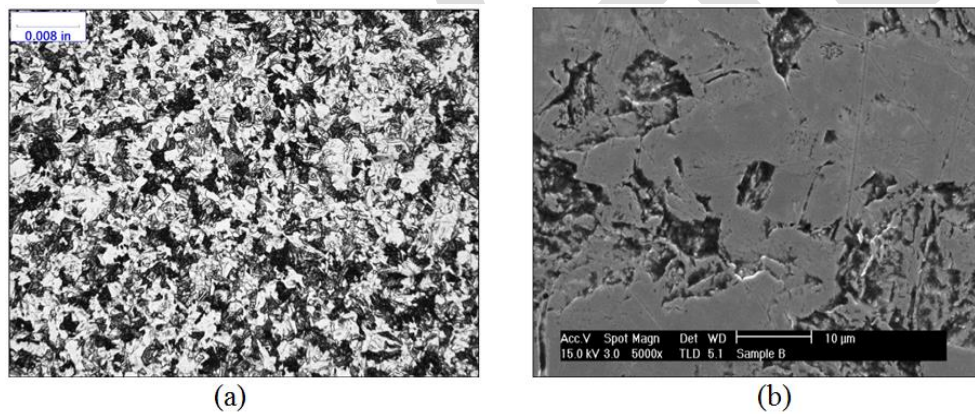


**Figure 5:** Microstructure of the normalized sample –a) LOM X200, b) SEM X5000

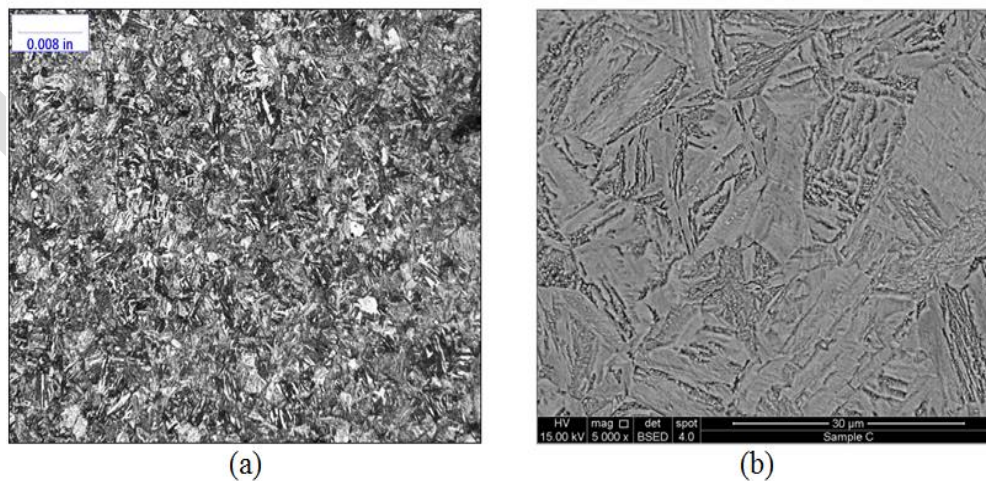


**Figure 6:** Microstructure of the austempered sample –a) LOM X200, b) SEM X5000

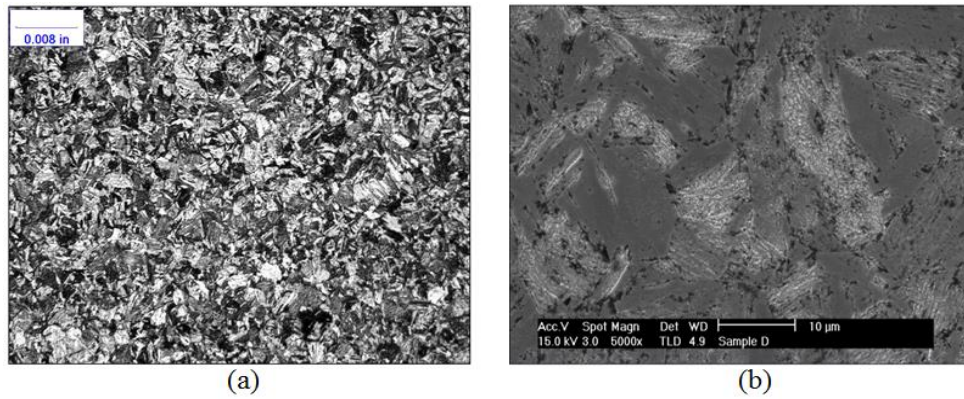


Figure 7: Microstructure of the quenched & tempered sample –a) LOM X200, b) SEM X5000

#### 4.2 Microstructure Impact on Mechanical Properties

Microstructure impact on fracture toughness was evaluated using J-integral testing. Fig 8 shows normalized microstructure indicated highest remarkable critical fracture toughness of  $373\text{kJ}/\text{m}^2$ , trailed by quenched and tempered ( $202\text{kJ}/\text{m}^2$ ), as-received ( $138\text{kJ}/\text{m}^2$ ) and then austempered microstructure ( $109\text{kJ}/\text{m}^2$ ). Soft pro-eutectoid ferrite matrix presence was responsible for the remarkable fracture toughness of normalization. The observation was in alignment with [11] the finding that steel impact toughness that had undergone normalization appeared tougher than austempered and quenched and tempered microstructure. But the austempered showed fracture toughness lower than the quenched and tempered due to presence of hard bainite matrix formation and possibly due to excessive retained austenite throughout the structure while the quenched and tempered exhibited higher level fracture toughness due to cementite precipitates, spheroidization and recrystallization ferrite matrix during tempering to  $550^\circ\text{C}$ . The toughness significant margin was not in alignment with [25] the recommendation to replace conventional quenching and tempering with austempering because of its better toughness owing to bainite-martensite or fully bainite structure composition.

Yield strengths were determined from stress-strain curves plotted on-line during tests. Comparative evaluation of the obtained yield strengths (Fig 9) indicated austempered microstructure has the highest yield strength of  $940\text{MPa}$ , followed by quenched and tempered ( $780\text{MPa}$ ), as-received ( $766\text{MPa}$ ) and normalized microstructure ( $408\text{MPa}$ ). The hardness results (Fig 10) showed marginal variation in the samples that had undergone different heat treatment methods in the same chronological order with yield strength which increased from austempered to normalization microstructure. The austempered microstructure showed highest average hardness value of  $318\text{Hv}$ , closely followed by quenched and tempered with  $251\text{Hv}$ , as-received ( $246\text{Hv}$ ) and normalized microstructure ( $192\text{Hv}$ ). The significant increase in the austempered yield strength and hardness values was attributed to hard constituent bainite sheaves and grain density formation in the structure which implied bainite appearance increases both yield strength and hardness of steel. But the quenched and tempered microstructure yield strength and hardness are slightly lower than the austempered despite tempering due to the presence of cementite formation in the martensite matrix which is a harder constituent than martensite. Contrastingly, the normalized sample indicated lowest yield strength and hardness values which suggested pro-eutectoid ferrite matrix and pearlite appearance in the microstructure were responsible for the obtained low values implying they are softer constituent compared with the bainite and martensite.

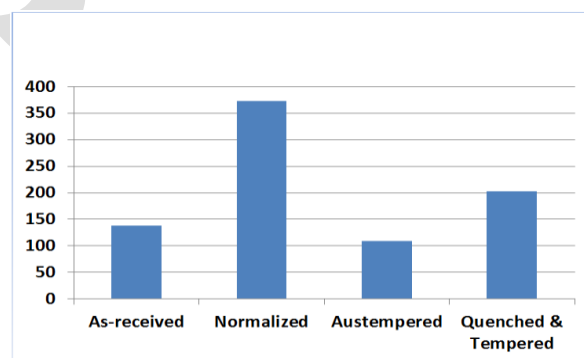
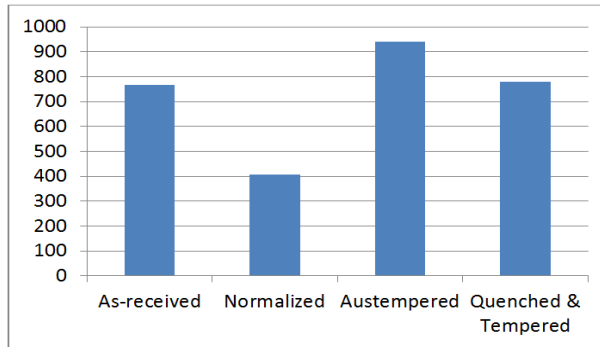
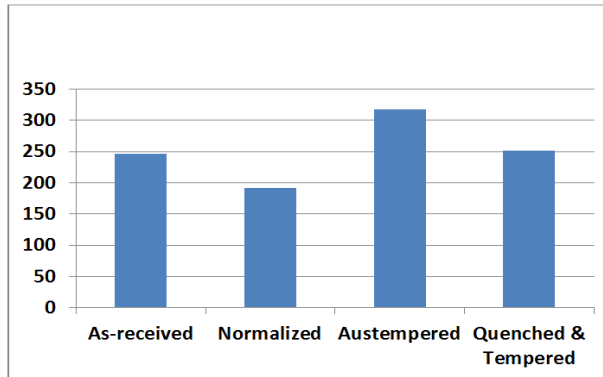


Figure 8: J-integral fracture toughness of microstructures chart



**Figure 9:** Yield strengths of microstructures chart



**Figure 10:** Vicker hardness of microstructures chart

## 5.0 CONCLUSION

The present study has shown that upper bainite structure with feathery and broad plate appearance could be formed at 350°C and not only within 500°C to 400°C depending on the isothermal holding period. Secondly, quenched and tempered microstructure indicated the best combination of fracture toughness, yield strength and hardness trade-off compared with normalization, austempered and as-received microstructures.

## REFERENCES:

- [1] J. Billingham, J. Healy, and H. Bolt “High strength steel- the significance of yield ratio and work hardening for structural performance” *Marine Research Review* Pub MTD, 1997.
- [2] B.S. Motagi and R. Bhosle “Effect of Heat Treatment on Microstructure and Mechanical Properties of Carbon Medium Steel” *International Journal of Engineering Research and Development*, Vol. 2, Issue 1, 2012, Pp 07 – 13.
- [3] E. Gogou “Use of High Strength Steel Grades for Economic Bridges Design”. *Master Thesis*, Delft University of technology, 2012.
- [4] L.W. Ma, X. Wu and X. Kenong “Microstructure and property of medium carbon steel processed by equal channel angular pressing” *Material forum* Vol. 32, 2008, Pub. Institute of materials engineering Australasia ltd.
- [5] S. Al-rubaiey, E. Anon and M.M. Hanoon “The influence of microstructure on the corrosion rate of carbon steel” *Engineering and Technological Journal*, vol.31, 2013, part (A) No 10.
- [6] T. P. Arasu, R. Dhanasekaran, S. P. Kumar and N. Srinivasan “Effect of Hardness and Microstructure on En 353 Steel by Heat Treatment” *International Journal of Engineering and Science*, vol 2, 2013, pp 01-05.
- [7] S. Danda “Effect of Induction Hardening on High Carbon Steel Forgings” *International Journal of Soft Computing and Engineering*, vol. 1, issue11, 2011, pp 01-05.
- [8] S. S. Sharma, K. Jagannath, C. Bhat, U. Achutha Kini, P.R. Prabhu, P.K. Jayashree and M.C Gowrishankar “3<sup>rd</sup> International Conference on Mechanical” *Automotive and Material Engineering*, 2013, Singapore



- [9] S.M.A Al-Qawabah, N. Alshabatat, and U.F. Al-Qawabeha "Effect of Annealing Temperature on the Microstructure, Microhardness, Mechanical Behavior and Impact Toughness of Low Carbon Steel Grade 45". *International Journal of Engineering Research and Application*, vol 2, 2012, pp1550-1553.
- [10] M. M. Tash "Effect of Hot Forging Reduction Ratio and Heat Treatment on Hardness, Impact Toughness and Microstructure of Carbon and Low Alloy Steel" *International Journal of Advanced Technology in Engineering and Science*, Vol. 3, Issue 3, 2015.
- [11] C.A. Reddy "Effect of holding temperature and time for austempering on impact toughness of medium carbon and high alloy steel" *International Journal of Computer Network and Security*, vol 3, 2013.
- [12] X. Lian "The Complex Phase Transformation of Austenite in High Strength lineup steels and its influence on the mechanical properties" Doctoral thesis, University of Pittsburgh, 2012.
- [13] O. O. Joseph<sup>\*1</sup>, O. O. Joseph<sup>\*2</sup>, R. O. Leramo and O. S. Ojudun "Effect of Heat Treatment on Microstructure and Mechanical Properties of SAE 1025 Steel: Analysis by one – way ANOVA" *J. Mater. Environ. Sci*, Vol. 6, 2015, Pp 101 – 106.
- [14] D.A. Fadare, T.G. Fadara and O. Y. Akanbi "Effect of Heat Treatment on Mechanical Properties and Microstructure of NST 37-2 Steel" *Journal of Minerals and Materials Characterization & Engineering*, Vol. 10, Issue 3, 2011.
- [15] M.S. Htun, S.T. Kyaw and K.T. Lwin "Effect of Heat Treatment on Microstructure and Mechanical Properties of Spring" *Journal of Metals, Materials and Mineral*, vol 18, 2008, pp 191 – 197.
- [16] ASM International, ASM Handbook: Heat Treatment, Vol. 4, American Society for Metals, Ohio, 1999.
- [17] ASTM E1820 "Standard test method for measurement of fracture toughness" Pub. ASTM International USA, 2010.
- [18] ASTM E8 "Standard Test Method for Tension Testing of Metallic Materials" Pub. ASTM International USA, 2012.
- [19] ASTM E92 "Standard Test Method for Vicker Hardness and Knoop Hardness of Metallic Materials" Pub ASTM International, 2016.
- [20] G. Mathers, Hardness Testing Part 1, Article of TWI, 2005, Pp 4 – 5.
- [21] C. Chen, Fei-Yi, L. Truan-Sheng, and C. Li-Hui "Microstructure and Mechanical Properties of Austempering Cr-Mo alloy steel". *Journal of Materials Transaction*, vol 5, 2013, pp 56 – 60.
- [22] J. D. Verhoeven "Fundamental of Physical Metallurgy" Pub. John Willey & Son, 1975.
- [23] W. Callister "Material Science and Engineering. An Integrated Approach" Second edition. Pub. John Wiley and sons, Inc, 2005.
- [24] D. H. Herring "Vacuum Heat Treatment: Principles, Practices and Application" Second Edition, Pub BNP Media, 2005.
- [25] J. Wen, Q. Li and Y. Long "Effect of Austempering and Mechanical Properties of GCr18Mo Steel" *Material Science Engineering A*, 2006, pp 251 – 253.